Designer pulsed beams for enhanced space–time focusing

Richard W. Ziolkowski

Electromagnetics Laboratory, Department of Electrical and Computer Engineering, The University of Arizona, Tucson, Arizona 85721

David B. Davidson

Department of Electrical and Electronics Engineering, University of Stellenbosch, Stellenbosch 7600, South Africa

Received July 13, 1993

We have demonstrated analytically and numerically that at least 10–100-fold enhancements in intensities for similar input energies can be achieved in the focal region of a thin dielectric lens by the use of pulsed beams specifically designed for that purpose.

Pulses that are less than 10 fs in duration and contain as few as 4 cycles can now be generated. If one considers a 1.0-mJ, 10-fs pulse focused to a 1.73-μm spot, the resulting intensity at the focus is approximately 1×10^{18} W/cm^2. This is just below the threshold of the domain where some researchers[1] have claimed that a variety of novel physical effects in laser–matter interaction could be studied experimentally. These effects include nonlinear (multiphoton) Compton scattering and the generation of large-amplitude waves to accelerate electrons. They deal with the relativistic response of electrons to the large field strengths present in such intense optical pulses. If there were a means to achieve a more intense focus with current systems, the desired intensity realm, 10^{19}–10^{21} W/cm^2, could be reached more quickly.

In analogy with known CW (i.e., time-harmonic or monochromatic) results,[2,3] we expect that the properties of a pulsed beam focused by a thin lens should reflect its far-field behavior. Ziolkowski[4] and Ziolkowski and Judkins[5] have shown that ultrawide-bandwidth (UWB) pulsed beams can be designed so that their maximum intensity properties are enhanced relative to their energy characteristics. Thus a properly designed lens-focused UWB pulsed beam should exhibit intensity enhancements similar to those achievable with an aperture-generated pulsed beam. If we assume that a circular aperture $\mathcal{A}$ of radius a in the plane $z = 0$ is driven everywhere with the Gaussian spatially tapered, arbitrary-time-signal, pulsed beam, $G(\rho, \phi, z = 0, t) = E_0 \exp(-\rho^2/w_0^2)F(t)$, where the time signal $F(t)$ has the Fourier transform $\tilde{F}(\omega)$, the effective frequency[4,5] ω_{rad} of the UWB pulsed beam radiated by this aperture reduces to

$$\omega_{\text{rad}}{}^2 = \frac{\int_{-\infty}^{\infty} dt |\partial F(t)/\partial t|^2}{\int_{-\infty}^{\infty} dt |F(t)|^2} = \frac{\int_{-\infty}^{\infty} d\omega \omega^2 |\tilde{F}(\omega)|^2}{\int_{-\infty}^{\infty} d\omega |\tilde{F}(\omega)|^2}. \quad (1)$$

This effective frequency ω_{rad} accounts for the spectral energies launched into the medium, particularly those reaching the far field. The Rayleigh distance of the radiated energy of the Gaussian pulsed beam generated by this aperture is $L_G = \pi w_0{}^2/\lambda_{\text{rad}}$, and the divergence of its energy profile is $\theta^G_{\text{enrg}} = \lambda_{\text{rad}}/(\pi w_0)$, where $\lambda_{\text{rad}} = 2\pi c/\omega_{\text{rad}}$. If a thin circular lens of focal length f is now introduced into the initial aperture, one can represent the effects of the lens by introducing its transfer function into the Huygens–Kirchhoff representation of the field generated by the aperture. At the center of the focal plane, where $z = f$ and $\rho = 0.0$, an explicit analytical expression for the resulting lens-directed pulsed-beam field is obtained[6]:

$$g(\rho = 0, \phi, z = f, t) \sim E_0 \frac{L_G}{f} \frac{1}{\omega_{\text{rad}}} \times \{1 - \exp[-(a/w_0)^2]\} \frac{\partial}{\partial t} F(t - f/c). \quad (2)$$

Thus, in general agreement with Sherman[7] and Bor and Horváth,[8] the behavior of the lens-directed pulsed beam at the focus depends on a retarded time derivative of the initial signal. The appearance of the time derivative in the far-field behavior of a pulsed beam has been established.[4,5]

More explicit statements about the focal region behavior can be obtained from relation (2). The input energy $\mathcal{E}_{\text{in}}$ along the axis is given by $\mathcal{E}_{\text{in}} = \int_{-\infty}^{\infty} dt |G(\rho = 0, \phi, z = 0, t)|^2$; the energy radiated along the propagation axis is $\mathcal{E}_{\text{rad}}(z) = \int_{-\infty}^{\infty} dt |g(\rho = 0, \phi, z, t)|^2$. Then the focal amplification factor $\mathcal{FA}_{\text{enrg}} \stackrel{\text{def}}{=} \mathcal{E}_{\text{rad}}(f)/\mathcal{E}$, which measures the energy concentration at the focus, is obtained from relation (2) as

$$\mathcal{FA}_{\text{enrg}} \approx \{1 - \exp[-(a/w_0)^2]\}^2 (L_G/f)^2. \quad (3)$$

Let $\max_t u(t)$ represent the operation of finding the maximum in time of the function $u(t)$. Again from relation (3), the focal amplification factor $\mathcal{FA}_{\text{int}} \stackrel{\text{def}}{=} \max_t |g(\rho = 0, \phi, z = f, t)|^2 / \max_t |G(\rho = 0, \phi, z = 0, t)|^2$, which measures the maximum intensity concentration at the focus, is

$$\mathcal{FA}_{\text{int}} \approx \Upsilon_{\text{int}} \mathcal{FA}_{\text{enrg}}, \quad (4)$$

where we have introduced the intensity enhancement factor

$$\Upsilon_{\text{int}} \equiv \frac{\max_t |\partial F(t)/\partial t|^2}{\omega_{\text{rad}}{}^2}. \quad (5)$$

0146-9592/94/040284-03$6.00/0

If $F(t)$ represents a monochromatic signal with $\omega = \omega_{rad}$, then one finds $\Upsilon_{int}^{CW} \equiv 1$ so that $\mathcal{FA}_{int}^{CW} = \mathcal{FA}_{enrg}^{CW}$. Therefore from relation (4) we find that if we design an UWB pulse that has the same energy in the focal region as does the corresponding CW signal, i.e., if we force $\mathcal{FA}_{enrg}^{UWB} = \mathcal{FA}_{enrg}^{CW}$, then the UWB and CW maximum beam intensities at the focus satisfy $\mathcal{FA}_{int}^{UWB} = \Upsilon_{int}^{UWB}\mathcal{FA}_{int}^{CW}$. Thus, depending on the design of the driving time signal $F_{UWB}(t)$, one could obtain a significant intensity enhancement at the focus if $\Upsilon_{int}^{UWB} \gg 1$. Correspondingly, it has also been shown[6] that the waist of the maximum intensity profile in the focal region can be designed to be narrower than the energy profile: $w_{int}(f) \leq w_{enrg}(f) \approx (f/L_G)w_0 = \theta_{enrg}^G f$.

The intensity enhancement factor [Eq. (5)] can be made greater than 1 if one increases the ratio of the maximum radiated intensity over time to the average radiated intensity in time (radiated energy), i.e., the point quantity, $\max_t|\partial F_{UWB}(t)/\partial t|^2$, must be made larger than the average quantity, ${\omega_{rad}}^2$. We have designed[6] a variety of pulses that achieve this condition. One such intensity enhancement (IE) pulse is given by

$$F_{IE}(t) = \begin{cases} -(1-x^2)^4 & x = -1.0 + t/T_1 \text{ for } 0 \leq t \leq T_1 \\ -1 + 2(1-x^2)^4 & x = (t-T_2)/(T_2-T_1) \text{ for } T_1 \leq t \leq T_2 \\ (1-x^2)^4 & x = (t-T_2)/(T_3-T_2) \text{ for } T_2 \leq t \leq T_3 \end{cases} \cdot \quad (6)$$

This pulse has a continuous time derivative everywhere; and if we set $T_1 = m\delta$, $T_2 - T_1 = \delta$, and $T_3 - T_2 = m\delta$ so that $T_3 = (2m+1)\delta$, we find numerically that for $\delta = 3.0$ fs and $m = 15$, the effective frequency is ${\omega_{rad,IE}}^2 = 6.564 \times 10^{28}$, so that $\lambda_{rad,IE} = 7.357$ μm, the time record length $T_3 = 93.0$ fs, and the intensity enhancement factor $\Upsilon_{int}^{IE} = 24.5$. Careful analysis[6] of the properties of this pulse indicates that the positive-to-negative switch time δ controls the size of the intensity enhancement factor. With this fact in mind, we consider a different case, in which $\delta = 0.25$ fs and $m = 88$, so that $\lambda_{rad,IE} = 1.412$ μm and $T_3 = 44.25$ fs. The intensity enhancement factor now becomes $\Upsilon_{int}^{IE} = 131.93$. Thus one can achieve a greater than 100-fold increase in the maximum intensity at the same energy in the focal region of a thin dielectric lens with a properly designed UWB pulse. Note that these results are realizable in any designated frequency regime simply by an appropriate change in the time scales.

A body-of-revolution finite-difference time-domain (BOR-FDTD) simulator,[6] which solves numerically the full-wave vector Maxwell's equations for this lens-focusing problem, was used to test these predictions. In particular, the intensity enhancement pulsed beam was compared with a lens-focused 10-cycle windowed CW driving signal, $F_{10\text{-cycle}}(t) = [1 - x(t)^2]^4 \sin[10(2\pi t/T)]$, and a lens-focused 1-cycle pulsed-beam initiated with the driving signal, $F_{1\text{-cycle}}(t) = -(16/T)x(t)[1 - x(t)^2]^3$ where the term $x(t) = 1 - 2t/T$ and T represents the total duration of the signal. For the 10-cycle CW pulse we found that ${\omega_{rad,IE}}^2 = 6.597 \times 10^{28}$, so that $\lambda_{rad,IE} = 7.339$ μm, $T = 245.233$ fs (i.e., 24.523 fs per cycle), and $\Upsilon_{int}^{IE} = 0.995$. For the 1-cycle pulse we found that ${\omega_{rad,IE}}^2 = 8.979 \times 10^{28}$, so that $\lambda_{rad,IE} = 6.290$ μm, $T = 24.523$ fs, and $\Upsilon_{int}^{IE} = 1.308$. The lens used in the BOR-FDTD simulations was double parabolic and thin. For all the numerical cases the lens was located at $z = 3.0$ μm; its thickness was $d = 2.25$ μm at its base, and its index of refraction was $n = 2$. The lens radius was $a = 9.0$ μm, giving a focal length of $f = a^2/[2d(n-1)] = 18.0$ μm and, hence, an f-number of 1.0. The waist of the initial Gaussian pulsed beam was set to $w_0 = 6.0$ μm.

The UWB IE, the 10-cycle, and the 1-cycle (normalized to one) pulses used in these simulations and their Fourier power spectra (normalized to the 10-cycle pulse's maximum) are shown in Figs. 1 and 2. Comparing these three signals, one finds that, even though they represent only a small portion of the total energy, the high-frequency components present in the UWB IE pulse play a significant role in the intensity enhancement. They allow the large intensity (instantaneous) values resulting from the time derivative to occur. The lower-frequency components nonetheless are providing significant amounts of energy to the focusing process—otherwise the

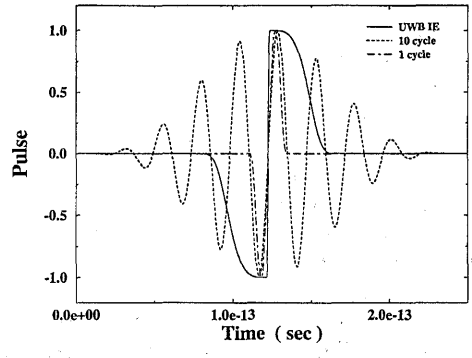

Fig. 1. UWB IE, the 10-cycle, and the 1-cycle pulses used in the lens-focused pulsed-beam simulations plotted as functions of time.

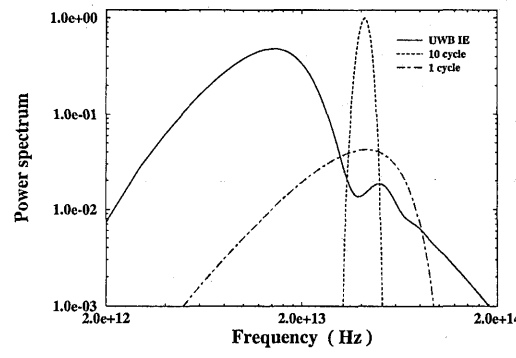

Fig. 2. Fourier power spectra of the UWB IE, the 10-cycle, and the 1-cycle pulses used in the lens-focused pulsed-beam simulations plotted as functions of the frequency.

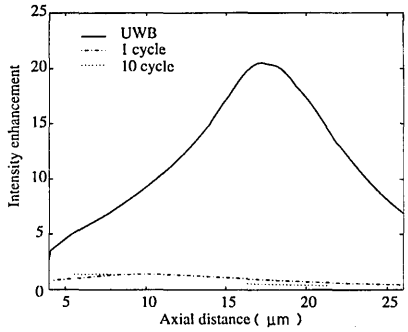

Fig. 3. Intensity enhancements near the focal region for the UWB IE, the 10-cycle, and the 1-cycle pulsed beams focused by the thin dielectric lens plotted as functions of the distance along the propagation axis.

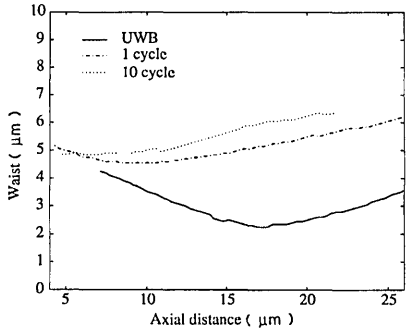

Fig. 4. Waists near the focal region of the UWB IE, the 10-cycle, and the 1-cycle pulsed beams focused by the thin dielectric lens plotted as functions of the distance along the propagation axis.

UWB IE pulsed beam could not achieve the same energy (average) value at the focus as the narrow-bandwidth 10-cycle pulsed beam or the broad-bandwidth 1-cycle pulsed beam. As in previous analyses,[4,5] we find that the higher-frequency components of a properly designed UWB pulsed beam act as a molasses that coheres the lower-frequency components to them as the entire pulsed beam propagates through the system.

These UWB IE, 10-cycle, and 1-cycle pulse values were chosen as an extreme comparison case to illustrate the dramatic differences between the intensity and energy behavior of an UWB pulsed beam in the focal region. The indicated parameters give $L_G/f = 0.86$ in the 10-cycle CW case and $L_G/f = 1.0$ in the 1-cycle CW case. These values indicate that the energy of the CW pulsed beams is not expected to experience any focusing effects in the focal region of the lens. The same energy behavior is expected in the UWB case. These energy behaviors were obtained with the BOR-FDTD simulator. After an initial redistribution of their energy by the lens and a slight focusing, the energy profiles of all the pulsed beams were expanding in the focal region of the lens as predicted. Moreover, the predicted time derivative behavior in the focal region was recovered in all cases.

The maximum intensity results obtained with the BOR-FDTD simulator are illustrated in Figs. 3 and 4. In Fig. 3 the intensity enhancements of the UWB IE, 10-cycle, and 1-cycle lens-focused pulsed beams are plotted as a function of the distance along the propagation axis. Note that noisy data in the 10-cycle case, which occurs in the numerical parameter extraction process, has been omitted simply to make the results clearer. Despite similar behavior for the energies of the lens-focused pulsed beams, there is a clear difference in the behavior of their maximum intensities. The numerical intensity enhancement factors at the focal plane $z = 17.2$ μm of the UWB IE pulse were $\Upsilon_{\text{int}}^{\text{10-cycle}} = 0.55$, $\Upsilon_{\text{int}}^{\text{1-cycle}} = 0.93$, and $\Upsilon_{\text{int}}^{\text{UWB}} = 20.52$. The maximum intensity enhancements, $\Upsilon_{\text{int}}^{\text{10-cycle}} = 1.52$ and $\Upsilon_{\text{int}}^{\text{1-cycle}} = 1.41$, for the 10-cycle and 1-cycle cases occurred near the lens and well away from the expected focal region. In Fig. 4 the corresponding waists of the maximum intensity profile are plotted. The maximum intensity profile waists in the UWB IE focal plane are $w_{\text{int}}^{\text{10-cycle}} = 6.0$ μm, $w_{\text{int}}^{\text{1-cycle}} = 5.15$ μm, and $w_{\text{int}}^{\text{UWB}} = 2.25$ μm. The agreement between the above numerical values for the intensity enhancement factors and waists and their analytical counterparts is very good. Similar results for 1-cycle, 10-cycle, and UWB IE cases with smaller λ_{rad} (hence, larger L_G/f factors to give energy focusing) are reported in Ref. 6.

The analytical and BOR-FDTD simulation results clearly demonstrate that one can achieve significantly enhanced behavior in the focal region with properly designed UWB pulses. Because the results in this Letter are scalable to any wavelength regime, we believe that optical experiments could be designed and performed to confirm the intensity enhancements reported here. Pulse shaping even in the subpicosecond regime has been reported recently.[9] On the other hand, the BOR-FDTD simulator results indicate that ultrashort, ultrasmall device structures in the femtosecond, micrometer-sized regimes can be used to achieve these effects. Practical applications for these UWB intensity enhancement systems may include particle acceleration, fiber-optic communications sources and detectors, and photolithography.

References

1. G. Mainfray, C. Manus, H. Brandi, T. Lehner, T. Auguste, and P. Monot, in *Programme et Resumes des Journées Maxwell,* J.-F. Eloi, ed. (CEA/CESTA, Bordeaux, 1993), p. 37.
2. J. J. Stamnes, *Waves in Focal Regions* (Hilger, Bristol, UK, 1986).
3. A. Yariv, *Quantum Electronics,* 2nd ed. (Wiley, New York, 1975), pp. 113–117.
4. R. W. Ziolkowski, IEEE Antennas Propag. **40,** 888 (1992).
5. R. W. Ziolkowski and J. B. Judkins, J. Opt. Soc. Am. A **9,** 2021 (1992).
6. D. B. Davidson and R. W. Ziolkowski, "Body-of-revolution finite-difference time-domain modeling of space–time focusing by a three-dimensional lens," J. Opt. Soc. Am. A (to be published).
7. G. C. Sherman, J. Opt. Soc. Am. A **6,** 1382 (1989).
8. Zs. Bor and Z. L. Horváth, Opt. Commun. **94,** 249 (1992).
9. A. M. Weiner, S. Oudin, D. E. Leaird, and D. H. Reitze, J. Opt. Soc. Am. A **10,** 1112 (1993).